RI 9117

Bureau of Mines Report of Investigations/1987

Analysis of Cutter Roof Failure Induced by Clastic Dikes in an Underground Coal Mine

By Eric R. Bauer and John L. Hill III

UNITED STATES DEPARTMENT OF THE INTERIOR

Report of Investigations 9117

Analysis of Cutter Roof Failure Induced by Clastic Dikes in an Underground Coal Mine

By Eric R. Bauer and John L. Hill III

UNITED STATES DEPARTMENT OF THE INTERIOR
Donald Paul Hodel, Secretary

BUREAU OF MINES
David S. Brown, Acting Director

Library of Congress Cataloging in Publication Data:

Bauer, Eric R.
Analysis of cutter roof failure induced by clastic dikes in an underground coal mine.

(Report of investigations / Bureau of Mines ; 9117)

Bibliography: p. **22-23**.

Supt. of Docs. no.: I 28.23: 9117.

1. Mine roof control. 2. Clay veins. 3. Coal mines and mining. I. Hill, John L. II. Title. III. Series: Report of investigations (United States. Bureau of Mines) ; 9117.

TN23.U43 [TN288] 622 s [622'.334] 87-600149

CONTENTS

ILLUSTRATIONS

ILLUSTRATIONS--Continued

TABLES

UNIT OF MEASURE ABBREVIATIONS USED IN THIS REPORT

ft	foot	pct	percent
ft^2	square foot	psi	pound per square inch
ft-lbf	foot pound (force)	psig	pound per square inch, gauge
in	inch		

ANALYSIS OF CUTTER ROOF FAILURE INDUCED BY CLASTIC DIKES IN AN UNDERGROUND COAL MINE

By Eric R. Bauer[1] and John L. Hill III[1]

ABSTRACT

Cutter roof failure, a ground control problem that frequently results in massive roof failure, is common in coal mines of the Northern Appalachian Coal Basin, causing delays in production and posing a safety hazard to mine personnel. The Bureau of Mines is conducting research on the causes of cutter roof failure to gain a basis from which to predict and prevent its occurrence, and to support such roof when failure occurs or is imminent.

Research conducted at the Greenwich Collieries North and South Mines, in central Pennsylvania revealed a correlation between the presence of clastic dikes and formation of cutter roof failure. The research consisted of in-mine mapping of geologic and deformational features, rock pressure monitoring, core recovery and evaluation, and in situ stress measurement. It was found that roof failure increased in areas where the occurrence of clastic dikes was most frequent, especially where two or more clastic dikes intersect.

Staggering of crosscuts prevented the extension of cutters and deterred the occurrence of large falls extending over several breakthroughs. In addition, trusses and cribbing were effective in stabilizing clastic dikes and inhibiting the development of cutter roof failure when employed immediately or shortly after mining.

[1]Mining engineer, Pittsburgh Research Center, Bureau of Mines, Pittsburgh, PA.

INTRODUCTION

Occurrences of cutter roof failure during development mining have been observed in increasing numbers. In response to this, the Bureau of Mines is investigating the causes of this type of roof failure, which can lead to a major roof fall if additional support is not utilized. The uniqueness of this problem has limited the techniques available for its treatment. Trial and error treatment has proven unsatisfactory in many cases, as the causes often differ from mine to mine.

Cutter roof failure begins as a fracture along one or both roof-rib lines of an entry or crosscut and propagates nearly vertically into the roof (fig. 1). When the fracture extends above the anchor horizon of the roof bolts, or deflects along a weak bedding plane, massive roof failure may occur. Figure 2 is an example of initial cutter failure, and figure 3 illustrates the end result of such cutter development.

Previous research by the Bureau has shown a correlation between cutter roof failure and high horizontal stress fields. Aggson (1)[2] and Kripakov (2) conducted studies using finite element analysis to address the particular stress state that would initiate cutter failure. Thomas (3) approached cutter development from a purely practical perspective and suggested that rock type was an important factor in the development of cutter failure. The influence of clastic dikes on cutter failure was reported by Moebs and Ellenberger (4), who proposed that clastic dikes should be expected where the immediate roof consists of thick, clay-rich rock, or immediately beneath other strata where the clay-rich layer has been removed by erosion. They also suggested the localized use of sealants or angle bolting to help prevent the associated roof problems. The influences of the direction of mining and occurrence of clastic dikes on cutter roof failure formation have been observed through detailed mapping by Iannacchione, Popp, and Rulli (5). Chase (6) investigated the physical characteristics and roof instability associated with clastic dikes in order to make support recommendations. Specifically, he addressed the cantilever effect that occurs during failure of clastic-dike-affected roof. A more comprehensive discussion of previous cutter roof research efforts is given by Hill (7).

Cutter roof failure has severely affected entry stability at the Greenwich Collieries North and South Mines of Indiana County, PA. The investigations conducted there contributed to an

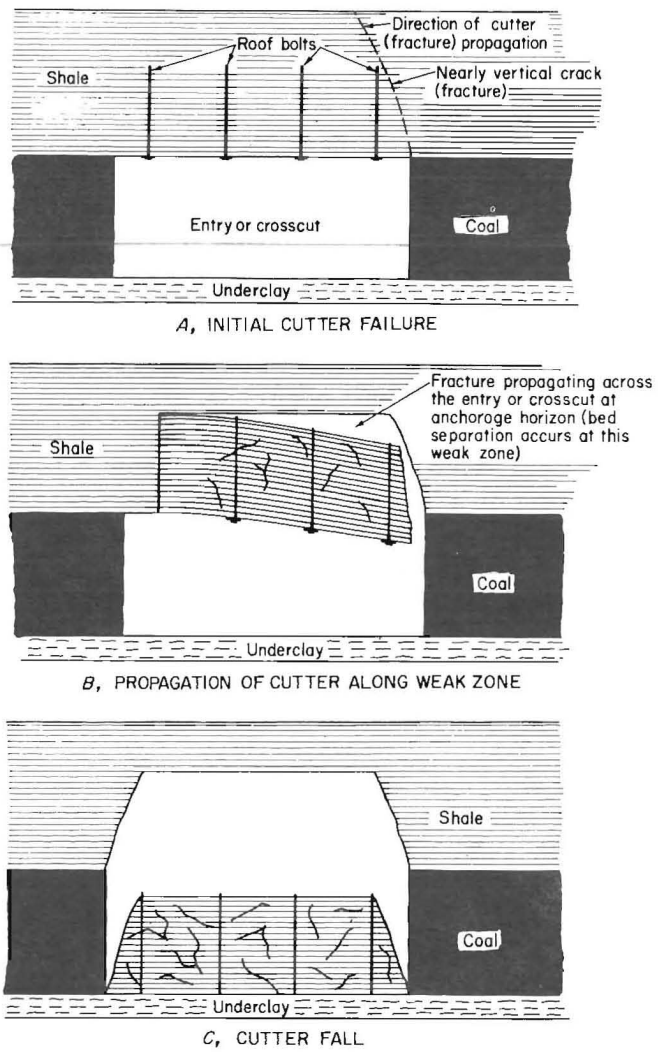

FIGURE 1.—Schematic of cutter roof failure sequence (8). Not to scale.

[2]Underlined numbers in parentheses refer to items in the list of references at the end of this report.

FIGURE 2.—Example of initial cutter roof failure.

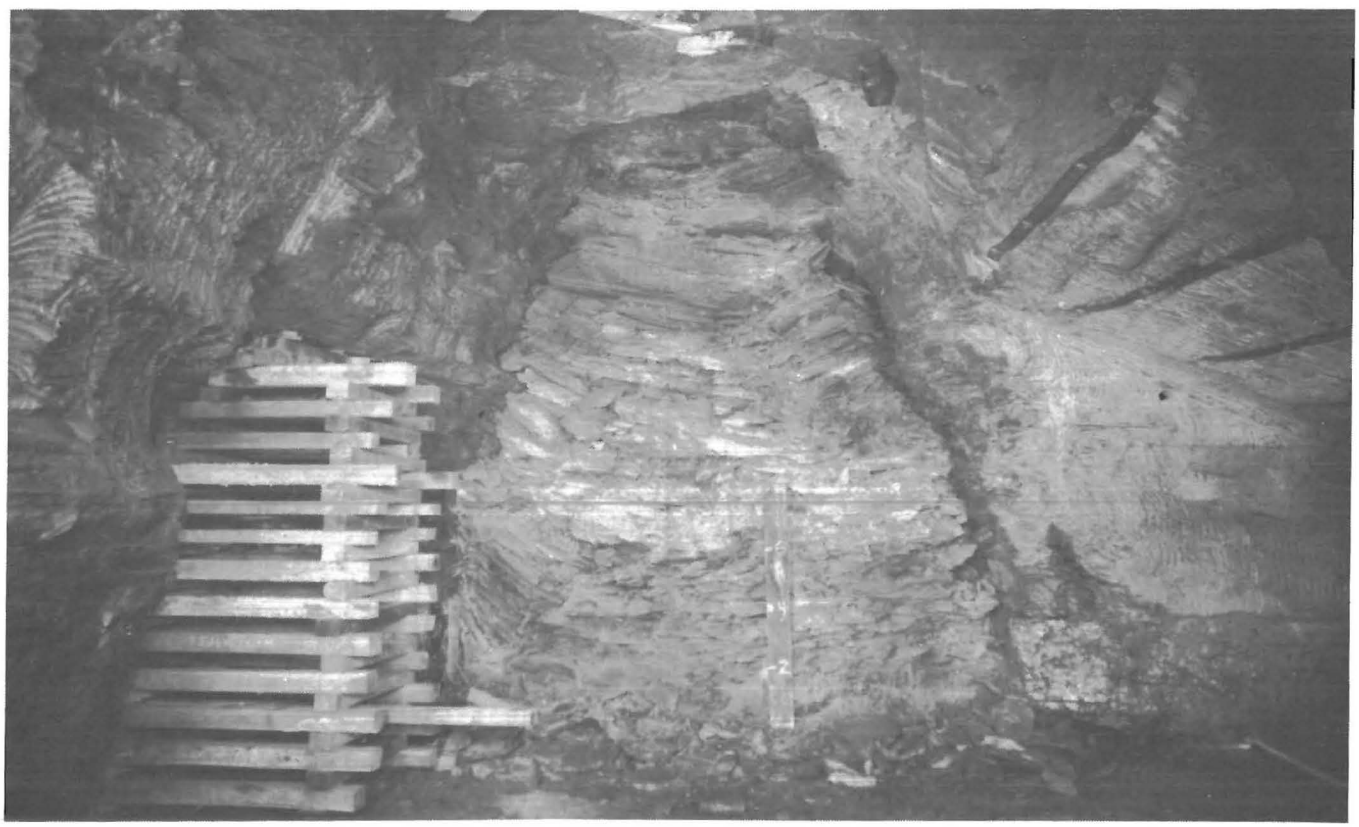

FIGURE 3.—Typical roof fall resulting from cutter failure (*8*).

understanding of the pressure dynamics surrounding cutter development and the influence of geologic anomalies, especially clastic dikes, on cutter roof formation. Clastic dikes are commonly known in mining terms as clay veins but are also referred to as clay or sedimentary dikes. A general definition of a clastic dike is a "sedimentary dike" consisting of a variety of broken rocks derived from overlying or underlying material.

Initially, a site-specific investigation was conducted in the Main A headings in the North Mine to verify that the presence of clastic dikes was the predominant cause of localized cutter failure (8-9). Then, detailed mapping of geologic and deformational features in both the North and South Mines was conducted to determine if the same mode of failure was present throughout the remainder of the two mines.

ACKNOWLEDGMENTS

The authors express their thanks to the officials and personnel of Greenwich Collieries North and South Mines, Pennsylvania Mines Corp., and Pennsylvania Power and Light Co. for their cooperation and assistance.

GEOLOGIC SETTING AND MINING METHOD

The study mines are located within the Appalachian Plateau Province in the broad trough of the Brush Valley Syncline (fig. 4). Structural relief on the mine property does not exceed 500 ft, and dips are generally less than 2.5°.

The coalbed being mined is the Lower Freeport (also known as the D seam), which is stratigraphically within the Pennsylvanian age coal-bearing Allegheny Group. At the study mines, the Lower

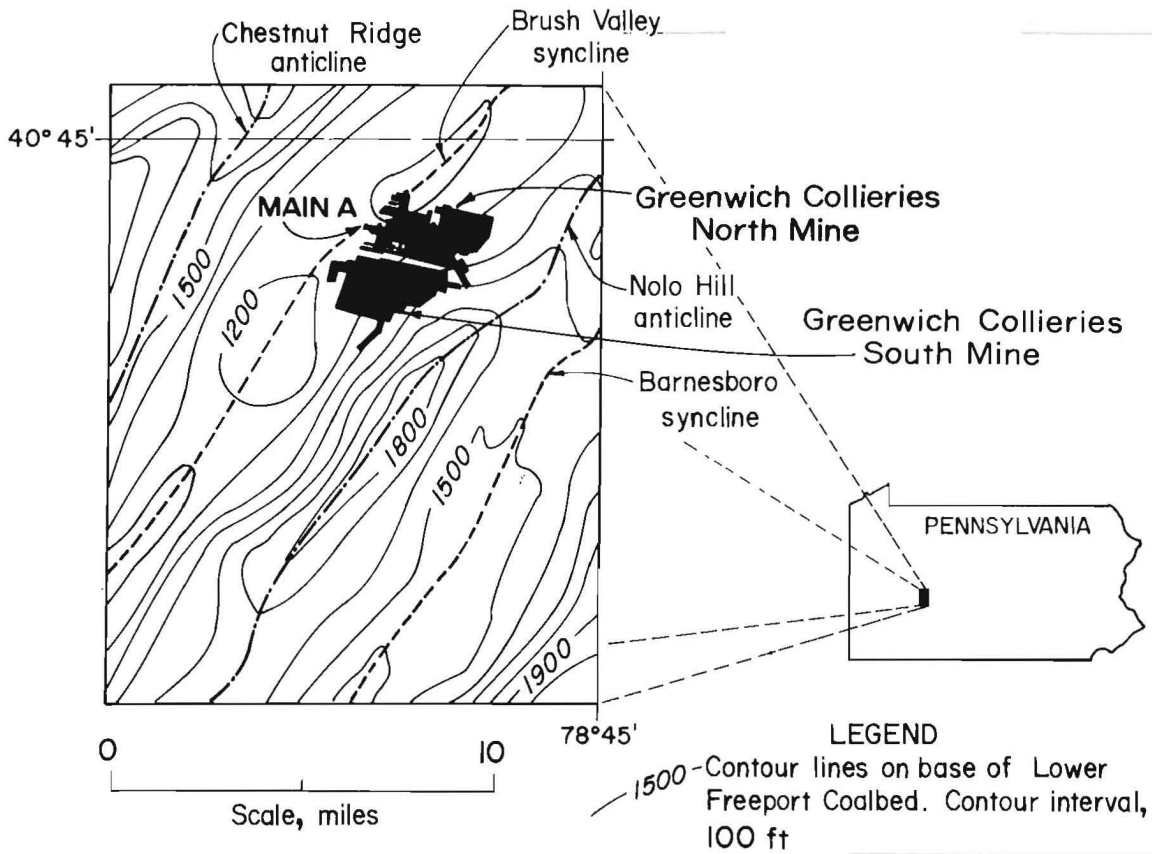

FIGURE 4.—Location of study mines.

Freeport Coalbed has an average thickness of 42 in and is directly overlain generally by 10 to 16 ft of a competent dark gray shale (fig. 5). Above the shale bed is a sandy shale interbedded with shale and sandstone (ranging from 10 to 13 ft in thickness), which can grade into a weak clayey shale approximately 20 ft above the coalbed. Intermittently, the channel-phase Butler Sandstone replaces the shale and sandy shale units. The next stratigraphically higher coalbed is the Upper Freeport with an average interburden of 30 ft. At the study mines the maximum overburden above the Lower Freeport Coalbed is 655 ft. Immediately below the Lower Freeport is a sporadically limy underclay ranging from 3 to 10 ft thick. This, in turn, is underlain by shale.

In general, the coal was extracted by the room-and-pillar mining system using a continuous miner, shuttle cars, and belt haulage. Main headings consisted of five to nine entries driven on 60-ft centers. Entry and crosscut widths were approximately 18 ft, with crosscuts normally driven on 80-ft centers.

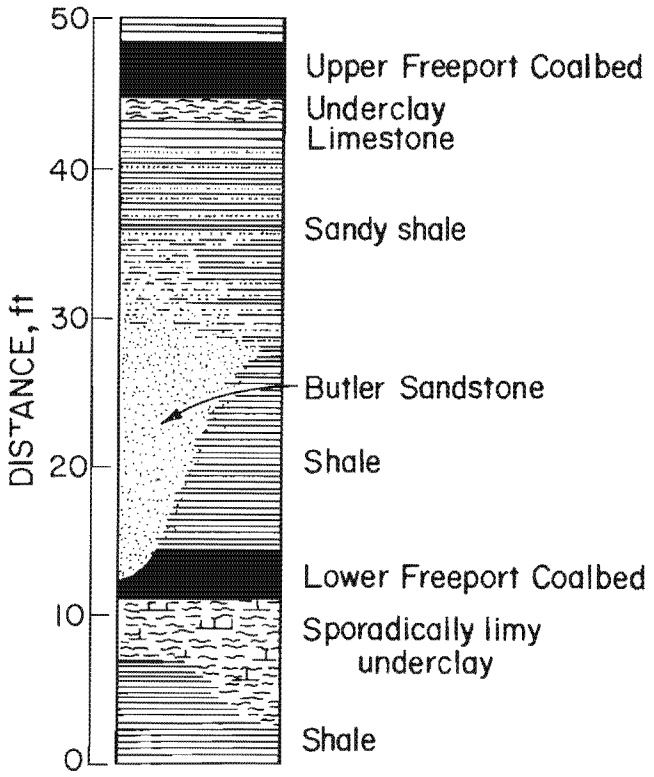

FIGURE 5.—Generalized stratigraphic column for the study mines.

INVESTIGATION OF MAIN A HEADINGS

Although cutter roof failure occurred throughout both mines, unusually severe cutter conditions were experienced near the face of the Main A heading (fig. 4). This heading will be used to reach the remaining reserves available to the North Mine; thus, it was important to maintain entry stability for the life of the mine. This site-specific investigation comprised four interrelated tasks: (1) in-mine mapping of all deformational and geologic features in the area studied, (2) coring of the mine roof and subsequent testing of the roof rock cores, (3) instrumentation of roof, pillars, and supports to determine pressure changes near and away from clastic dikes as mining advanced, and (4) measurement of the in situ horizontal roof stresses in the area most affected by cutter failure.

ASSESSMENT OF GROUND CONDITIONS

Detailed mapping of geologic features and deformation during cutter development was conducted in the Main A headings from the shaft to the face. Figure 6 is an example of the mapping and illustrates the relation of geologic features to roof failure. Clastic dikes (or clay veins), ranging in thickness from 1 ft of claystone matrix with fragments of shale and coal to a thin film of calcite or clay, are the primary roof-failure-initiating geologic features. Clastic dikes in areas overlain by channel and splay sandstones were filled with fine sand and silt instead of claystone. In some instances, infilled fractures and joints were by accident labeled clastic dikes because of similar appearance. The dikes

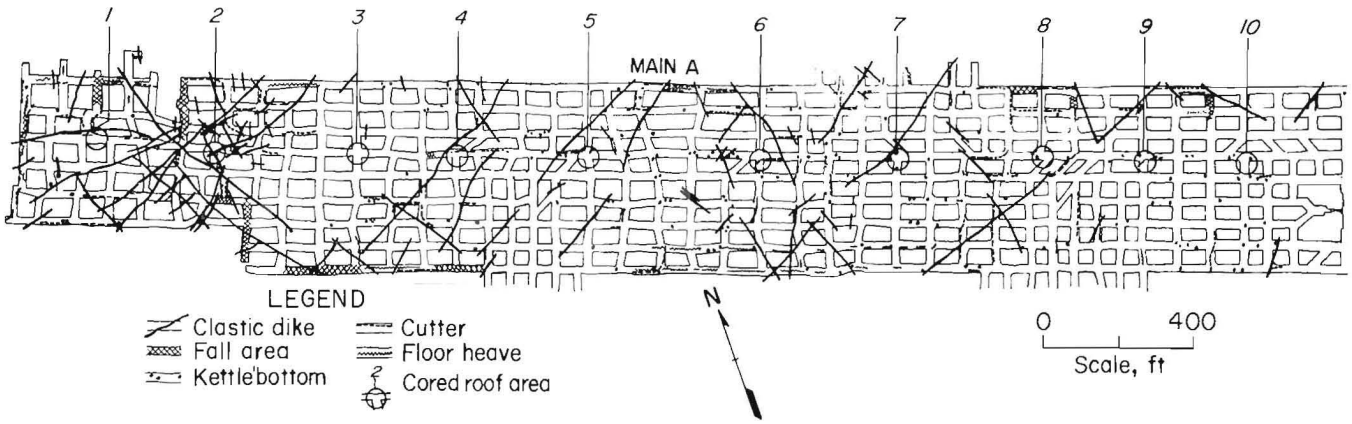

FIGURE 6.—Results of detailed mapping of the Main A headings (*9*).

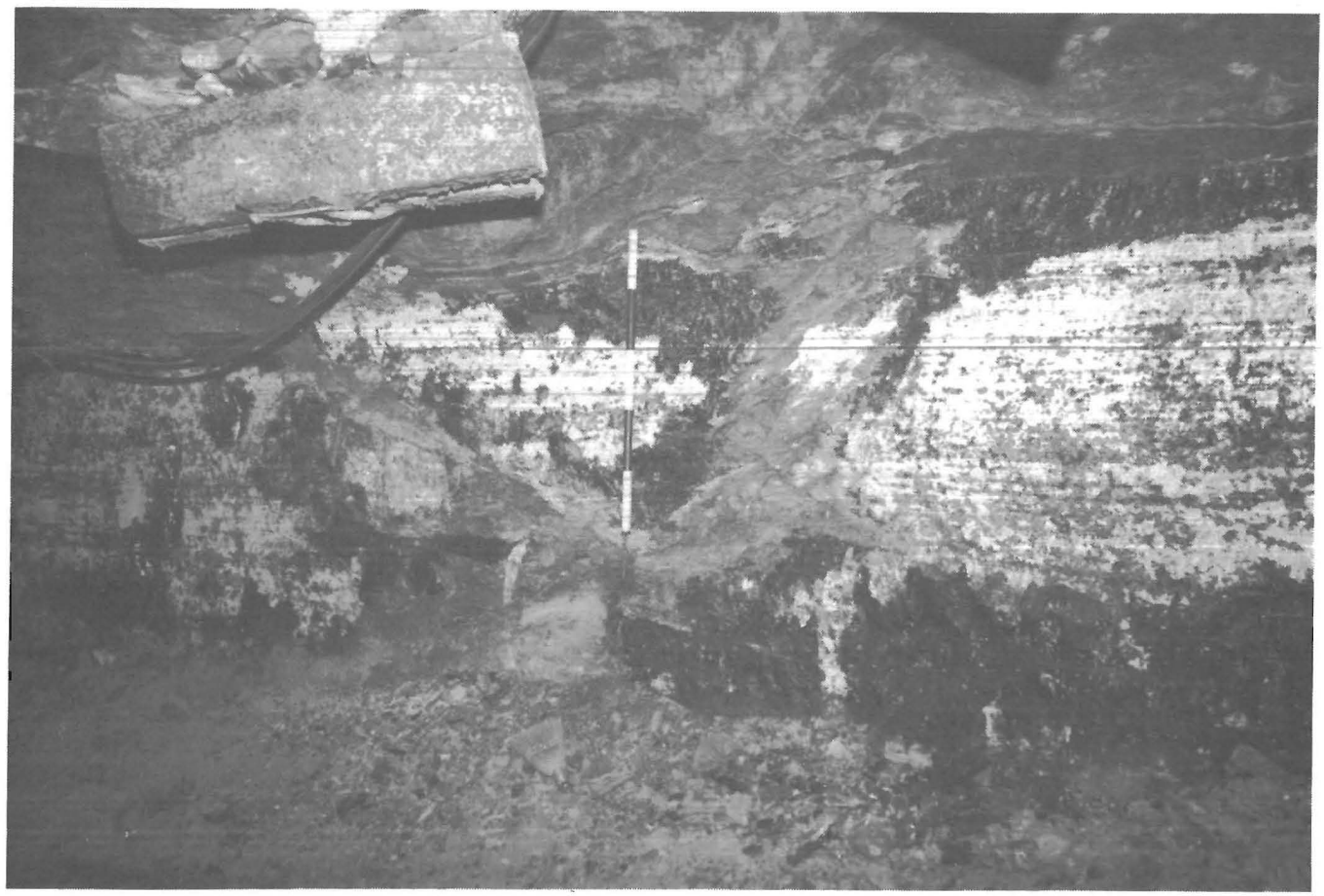

FIGURE 7.—Example of a clastic dike in both the mine roof and coal seam. (Courtesy F. E. Chase, BuMines, Pittsburgh, PA.)

exposed in roof falls extend as high as 26 ft into the roof rock and penetrate the coalbed at various angles. Figure 7 is an example of a clastic dike that has intersected both the mine roof and the coal seam. Few dikes reached the floor rock, suggesting an intrusion from above the coalbed. Fractures and slickensides in the roof were associated with clastic dikes, and slickensided surfaces were often marked with horizontal striations.

The character of the dikes suggests that they were formed through the simple infilling of fissures that resulted from

compressive, tensile, or shear ground failures. The fissures responsible for dike formation can be propagated either by compactional forces during the coalification process or by tectonic (regional or mountain building) stresses. The infilling of the fissures occurs primarily by the deposition of sediments from gravity or downward-percolating ground water (6).

Figure 8 is a histogram of the orientations of the clastic dikes found in the Main A headings. A bimodal distribution of N 35° W and N 55° E existed, possibly due to the proximity of the syncline and the stress field present during dike formation. This bimodal distribution is significant because it is different from the orientations of the Main A entries and crosscuts, which are N 75° W and N 15° E, respectively. Although oriented for reasons other than control of the problems related to clastic dikes, Main A is being driven at a heading that minimizes the dikes' effects on roof instability.

Nearly 75 pct of all cutter failure was found to abut a clastic dike; penetration into the roof (often greater than 2 ft) was deepest directly next to the dike, decreasing as the distance from the dike

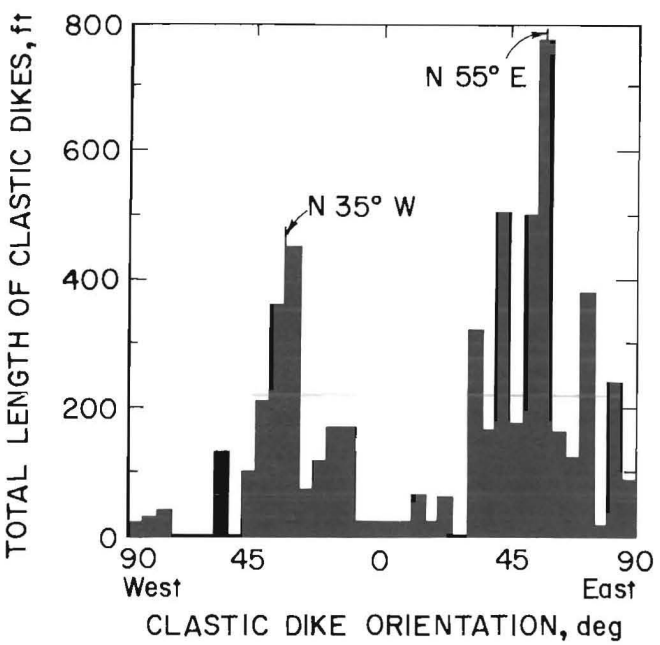

FIGURE 8.—Histogram of clastic dike orientations in the Main A headings from the shaft to the face.

increased. This suggests that cutter failure was facilitated by the clastic dikes and the manner in which they disrupt roof integrity. The disruption of roof integrity and the failure sequence are described in detail in the "Roof Failure Analysis" section later in this report. In fact, cutter failure was witnessed to initiate at the intersection of a clastic dike with the rib. When cutter failure progressed enough to cause roof falls, clastic dikes often formed the boundaries of the fall area.

Figure 9 shows that the frequencies of clastic dikes and cutters were much greater near the face of Main A than near the shaft area. Main A was divided into seven equal areas of 87,000 ft^2 from the face to the shaft. The total lengths of clastic dikes, cutters, and roof falls in each area were calculated, then plotted on a histogram (fig. 10). This histogram shows that there was a gradual increase of both clastic dikes and cutters from the shaft to the face. Along with the increase in dikes and cutters is a corresponding increase in roof falls, a normally occurring and predictable trend. Also plotted on figure 10 is the total number of kettlebottoms found in each area. Kettlebottoms were found in all areas of the Main A headings, indicating that generally similar environmental conditions were present during coal formation of the entire area. The entirety of the mapping suggests that the stresses were greater in the area of the present mining face at some point in time, possibly due to the formation of the syncline causing more fissures and eventually, through infilling, more clastic dikes.

Other geologic features such as fractures, joints, and cleat were mapped but appeared to have no major influence on entry stability. The only other deformational feature found in the Main A headings was floor heave. As can be seen from figure 6, floor heave occurred in entries and crosscuts adjacent to the solid coal. This is believed to be due to high abutment pressures in these outer entries, although no attempt was made to verify this observation through extensive instrumentation.

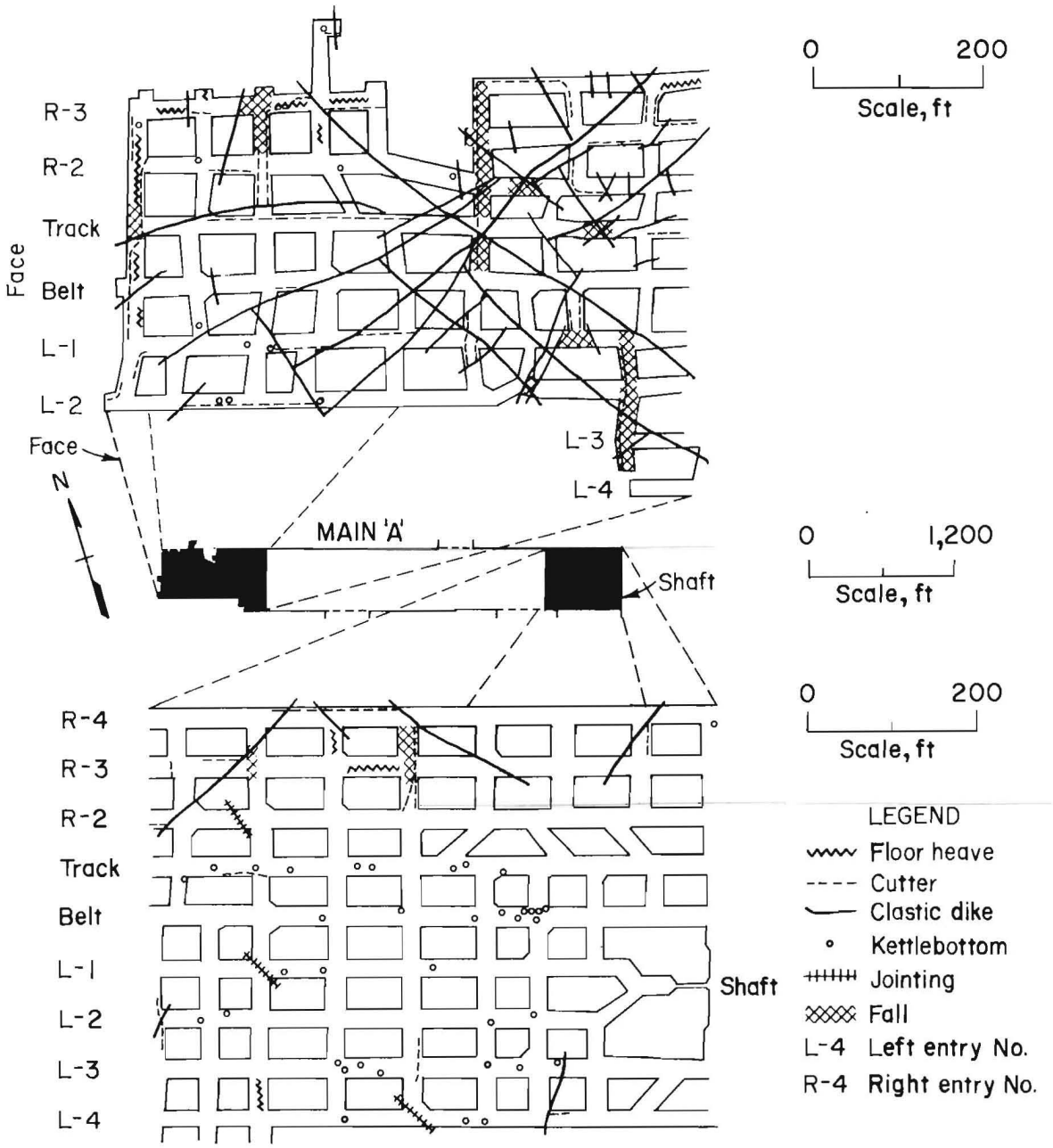

FIGURE 9.—Comparison of the geologic and deformational features in the face area and shaft area of the Main A headings (*8*).

ROCK MASS CHARACTERISTICS

Ten locations for coring the roof rock were selected, roughly equally spaced between the shaft and face (fig. 6) of Main A, to obtain an overall picture of rock mass characteristics. Rock was cored to a height of 10 ft above the coalbed-roof rock interface to ensure analysis of the rock mass through and above the roof bolt anchor horizon. Additional core was obtained during measurement of in situ stresses when roof rock was cored to a height of 22 ft above the coalbed. The core was logged with respect to lithology and fractures, and then subjected to mechanical property testing.

Roof Fracture Analysis

To relate fracture to roof stability, the fracture data were converted to a unit devised by Deere (10) known as Rock

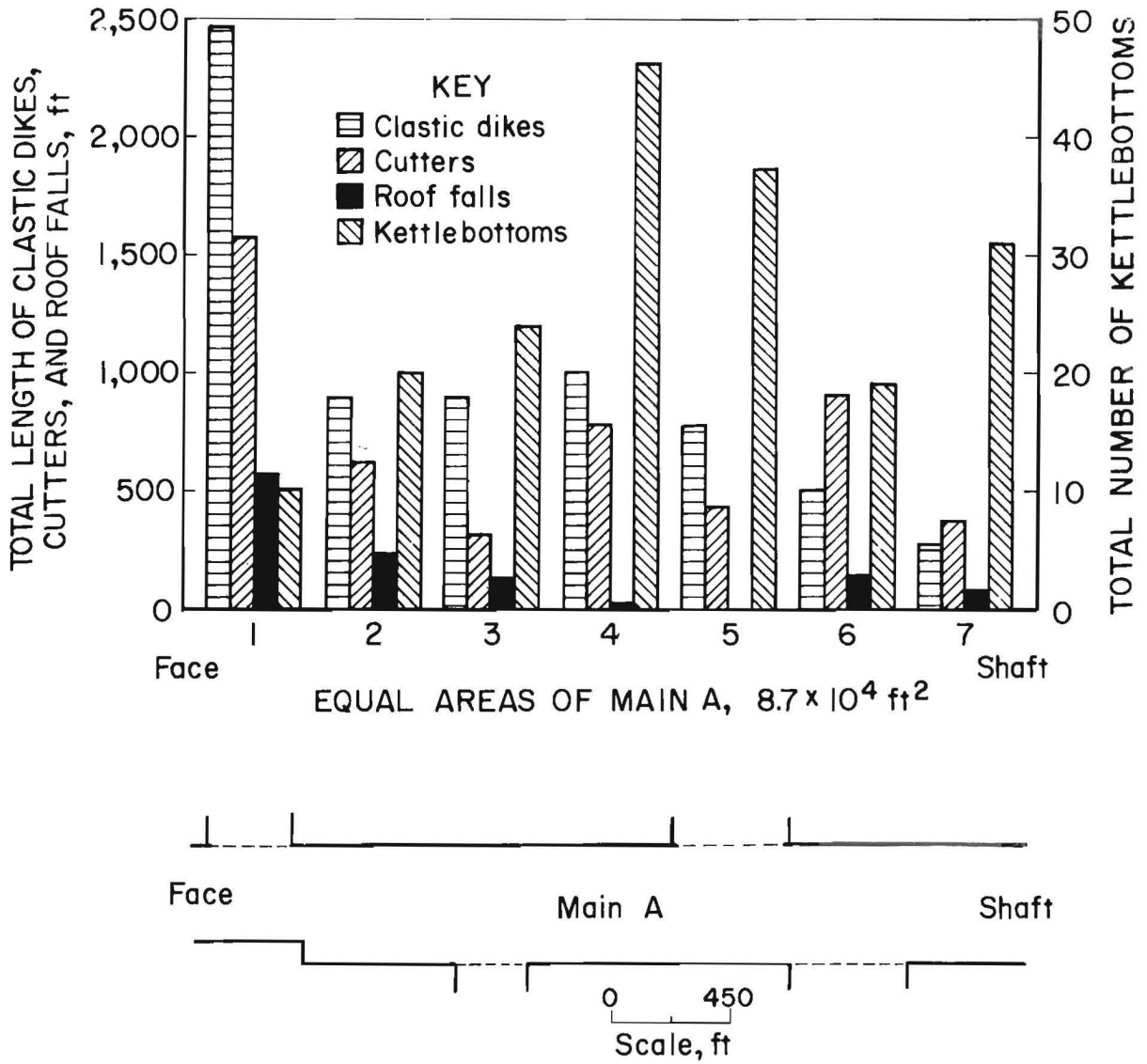

FIGURE 10.—Histogram of the geologic and deformational features in the Main A headings from the shaft to the face.

Quality Designation (RQD); this is a common method used to describe rock stability. The RQD data were then related to coal mine roof stability through the use of a technique developed by Kalia (11), which is a correlation between RQD and roof support requirements for coal mines as listed in table 1. Since 6-ft point anchor resin, tension-rebar-type roof bolts were used in the Main A headings, it was advantageous to look at the RQD data in four different ways: the overall value for each hole, to give an indication of roof stability; and then for each third of the hole, to analyze below the anchor horizon of the bolts, in the

TABLE 1. - Correlation between RQD and roof support requirements for coal mines

RQD, pct	Rock quality	Support requirements
0-25...	Very poor	Heavy steel, long bolts.
25-50..	Poor.....	Do.
50-75..	Fair.....	Do.
75-90..	Good.....	Light to heavy steel, pattern bolts.
90-100.	Excellent	Unsupported or occasional bolts.

Source: Modified from Kalia (11).

TABLE 2. - RQD data for each cored hole, percent

Location[1]	1	2	3	4	5	6	7	8	9	10
Overall.	71	55	93	93	75	60	71	74	52	78
Bottom..	NA	NA	NA	NA	45	45	36	86	22	82
Middle..	50	0	93	100	97	47	83	66	44	66
Top.....	94	100	93	88	82	82	91	70	87	83

NA Data not available because roof rock was mined at these locations.

[1]Bottom, middle, and top refer to each third of a hole.

anchor horizon, and above the anchor horizon (table 2).

Two distinct correlations were found between RQD and roof conditions. First, when the overall RQD values for each hole were compared with mapped geologic and deformational features around the hole, a relation was seen between holes with low RQD values and the proximity to a clastic dike or cutter failure (figs. 6 and 11). Second, a relation was seen between low RQD values in areas of each corehole and the presence of a carbonaceous sandy shale which was consistently present in each hole approximately 5 ft above the coalbed. By combining these two correlations, the data suggest that roof bolts longer than 5 ft should be used, to ensure a solid anchor above the fractured zone. Based upon the Kalia system, maximum support should be employed when clastic dikes are present or where cutter failure has occurred, since the data also show low RQD values for these areas.

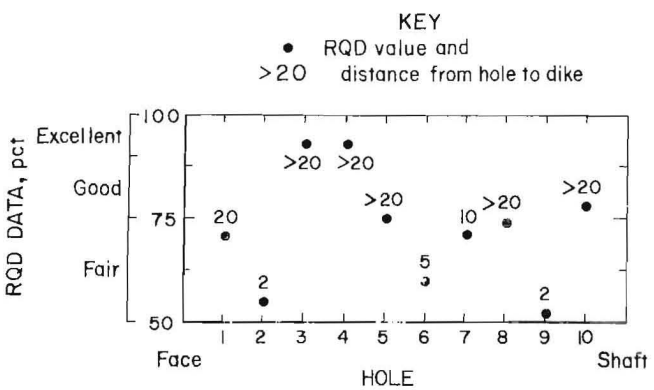

FIGURE 11.—RQD data accompanied by a number indicating the distance from the cored hole to a clastic dike or cutter failure in feet (9).

Otherwise, the roof is stable according to the Kalia system and should require only normal patterned bolting. The mapping of clastic dikes and cutter failure throughout the Main A headings supports these recommendations.

Rock Strength and Material Property Analysis

The next phase of the rock analysis consisted of rock strength testing of the logged core. Under normal core recovery conditions, uniaxial compressive strength and tensile strength tests would be conducted to compare the strength of the roof rock. However, owing to the short lengths of core recovered from the initial 10 coreholes, the necessary 2:1 ratio of length to diameter needed for uniaxial strength tests was not frequently obtained. Thus, the point load testing method, as described by Broch and Franklin (12) with slight modifications as described by Bauer (13) and Fitzhardinge (14), was used for comparing the relative strength of the immediate roof rock at each corehole location. When core lengths of 2:1 were available, the more standard tests were conducted.

It seemed desirable to have a measure of the anisotropic nature of the rock in addition to the basic rock strength because the rock being tested was shale. The core specimens were thus subjected to axial and diametral point load tests. As figure 12 shows, rock strength, measured by Broch and Franklin's axial strength index (12), varied very little overall for each hole from one end of the main entry system to the other. The average strength value of 6.2 for the entire unit is well within the "very strong"

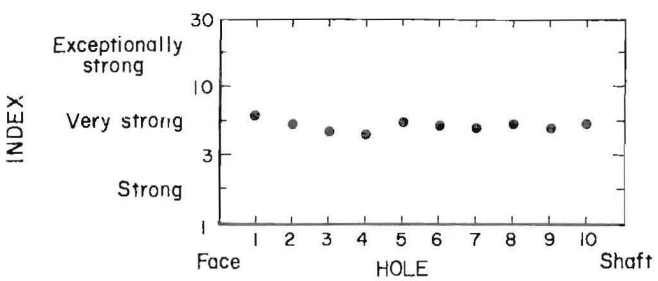

FIGURE 12.—Axial strength index values for each corehole. (9).

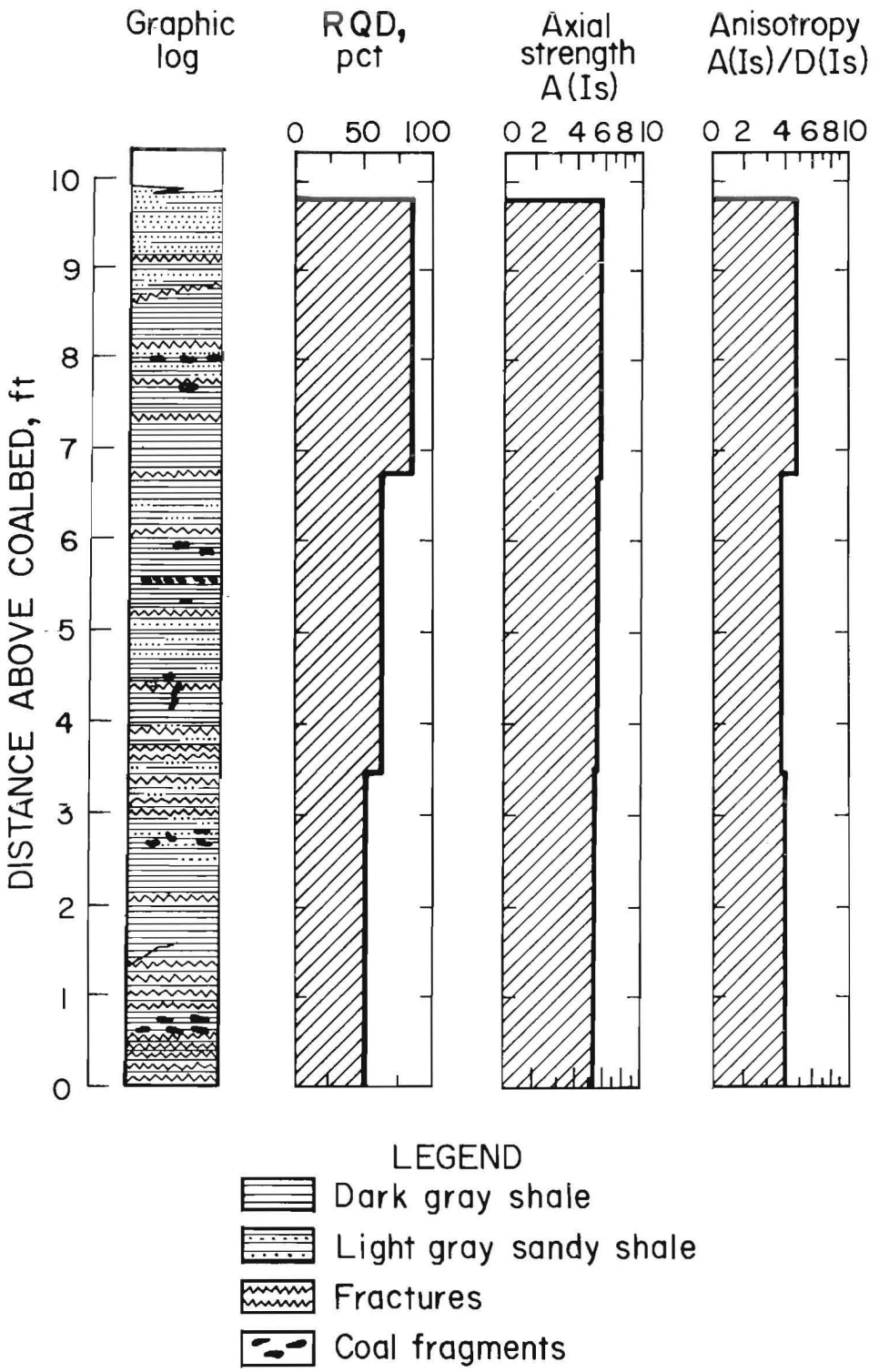

FIGURE 13.—Generalized stratigraphic column and rock properties in the Main A roof. Note: D(Is) in the diametral strength of a specimen determined from point load tests.

designation. Figure 13 is a cumulative diagram of the assessment made of the immediate 10 ft of roof rock. The stratigraphic column, RQD, axial strength, and anisotropic value are all averaged values to represent the entire main entry system from the shaft to the face. In general, the roof rock was comprised of two rock types within this 10-ft interval: a dark gray shale with an average compressive strength of 13,380 psi, and a light gray sandy shale with an average compressive strength of 15,280 psi.

Triaxial compression tests were performed on the dark gray shale, which comprises the lowermost member of the immediate roof. The tests yielded a cohesion shear strength of 4,820 psi, and a phi angle of 26°. This high value for shear strength and the phi angle are similar to the results obtained by Aggson as reported by Kripakov (2) for the Kitt Mine of West Virginia, where cutter roof failure is a chronic condition. Others have also cited competent immediate roof strata as a necessary condition for the initiation of cutter roof failure (3, 15).

Figure 14 is a stratigraphic column of the roof rock at the corehole where the in situ stress measurements were taken.

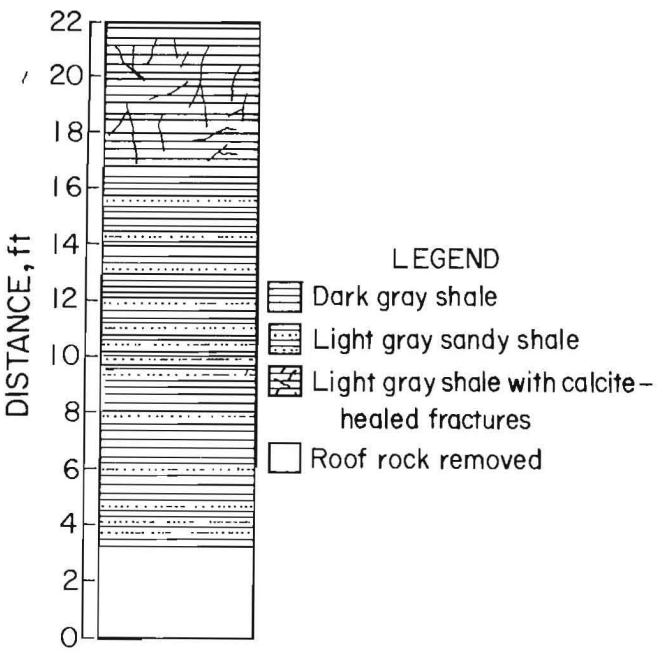

FIGURE 14.—Stratigraphic column of the roof rock at the in situ stress measurement site.

The immediate 10 ft of roof rock was identical in its characteristics to that from the other 10 coreholes, but 16.75 ft above the coalbed a light gray shale was present, which was highly fractured and healed with calcite infilling. This rock unit continued to the top of the corehole, which was 21.33 ft above the coalbed. The compressive strength of this material was very low, averaging 4,160 psi. Young's modulus and Poisson's ratio were calculated from the specimens for use in calculating in situ stress. The fractured nature of the specimens resulted in strain hardening during compression tests. The average tangent value of Young's modulus was 2.01×10^6 psi, and the average tangent value of Poisson's ratio was 0.33.

ROCK AND SUPPORT PRESSURE MONITORING

To measure and quantify the pressure dynamics associated with cutter roof failure, borehole platened flatjacks (BPF's), roof bolt U-cells, and flat hydraulic cells were employed. BPF's were placed in the roof strata to measure the pressure (shear slip) accompanying roof beam deflection. Since individual BPF's measure pressure changes in only one direction (16), two BPF's were used to measure mutually perpendicular horizontal pressure changes (parallel and perpendicular to the entries or crosscuts). The BPF's were set in the roof strata to a height of 3 ft from the mine roof surface, which placed them approximately halfway between the roof bolt anchor horizon and the mine roof surface. They had an initial setting pressure of approximately 260 psig to ensure a solid contact with the strata. The pressure was read as gauge pressure because barometric pressure was not considered to cause significant change.

Hydraulic U-cells were placed on roof bolts to measure bolt load (tension) changes. The flat hydraulic cells were used to monitor the loading on steel-fiber-reinforced concrete cribs that resulted from roofbeam deflection. The U-cells were installed on the regular mining cycle as the bolts were installed; their installation pressure was

controlled by the amount of torque applied by the bolting machine. This torque ranged from 200 to 300 ft·lbf, resulting in a U-cell reading of 575 to 725 psig. All BPF's and U-cells were installed in fresh cuts at the farthest advance of mining in each particular entry or crosscut. The flat hydraulic cells were placed on the cribs as the cribs were installed as supplemental support.

The first area monitored was in the L-1 entry of Main A; two BPF's were installed (fig. 15*A*). At the time of installation no cutter had formed in the entry, and the clastic dike to the west of the BPF's had not been exposed by mining. Approximately 3 days later, loading of BPF 1 began, as mining exposed a clastic dike just inby the BPF's. BPF 1 measured pressure changes perpendicular to the heading of the entry. Six days later, both BPF's showed signs of increased loading as a cutter began to develop adjacent to the clastic dike just inby the BPF's (fig. 16). As the cutter progressed to the next outby clastic dike, the loading on BPF 1 continued to increase. By day 10, posts were installed for additional support. However, loading continued to increase on both BPF's, and roof conditions continued to deteriorate. On day 30, the entire entry had to be cribbed to control the roof. Loading eventually leveled off as the cribs took

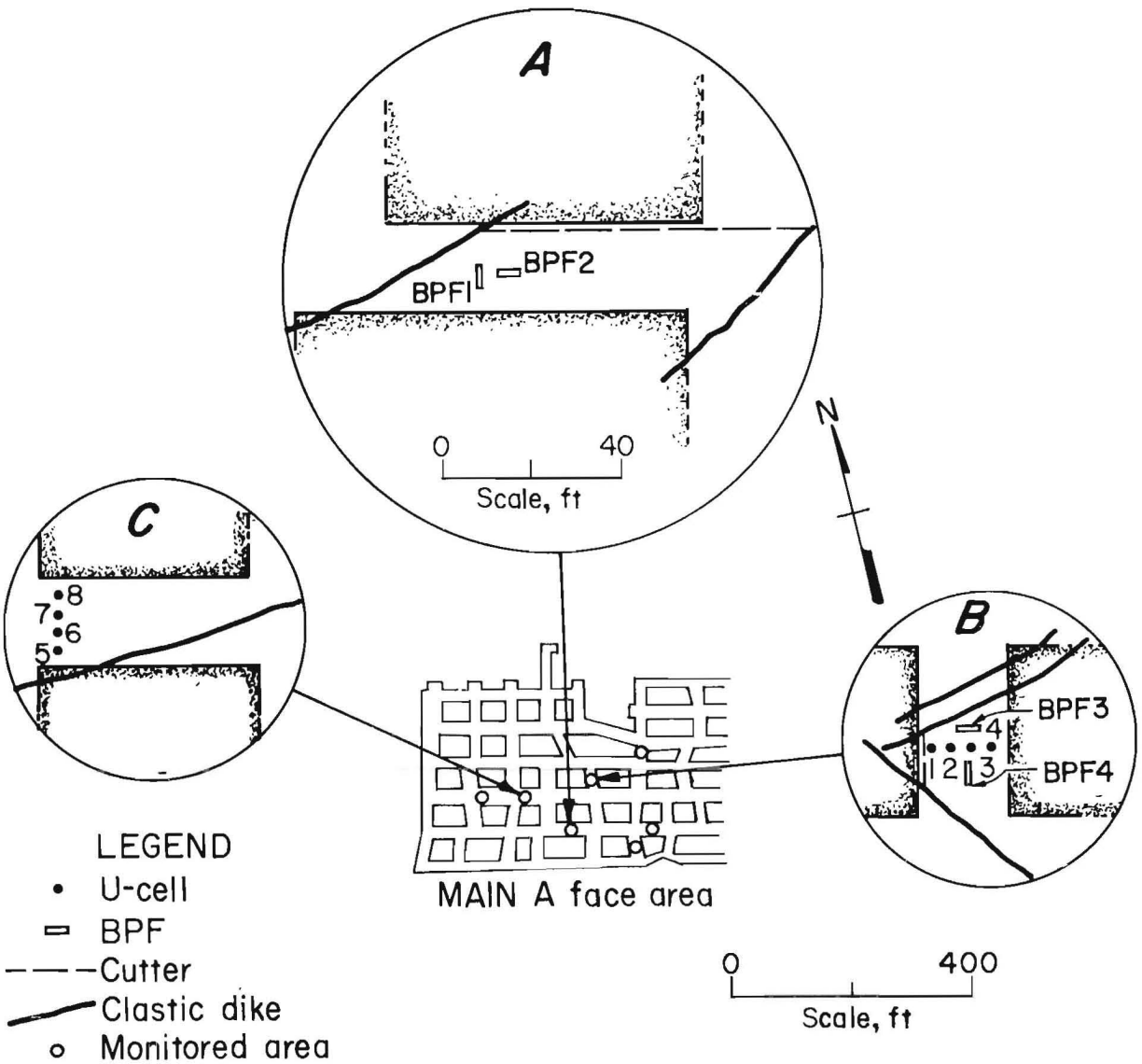

FIGURE 15.—Location map of monitored areas (*8*).

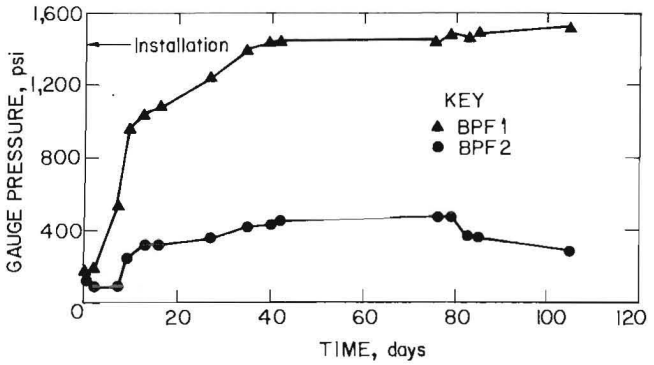

FIGURE 16.—Pressure monitoring behavior of BPF's 1 and 2 (*8*).

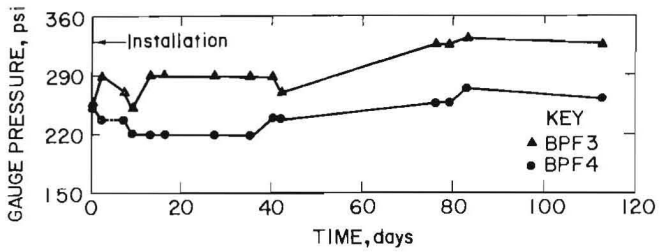

FIGURE 17.—Pressure monitoring behavior of BPF's 3 and 4 (*8*).

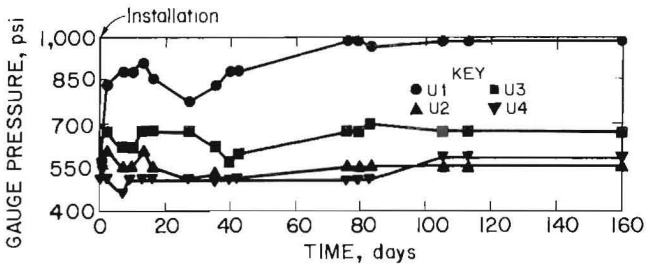

FIGURE 18.—Bolt load monitoring behavior of U-cells 1-4 (*8*).

the load, and the entry finally stabilized. Both BPF's responded as if the roof was acting as a cantilever beam with support on the southern pillar and the cutter along the northern pillar allowing the beam of the roof to bend. The cantilever beam effect is explained in detail in the "Roof Failure Analysis" section of this report.

The second area monitored was a crosscut between the belt and track entry (fig. 15*B*). The clastic dikes just north of the BPF's had not yet been exposed by mining, prior to installation of the instrumentation. Based on the first experience of monitoring cutter development, it was decided that U-cells would be installed on a row of bolts across the entry to measure bolt loading in addition to using BPF's.

Loading of U-cell 1 and BPF 3 occurred as soon as the next 20-ft cut into the face was taken from the crosscut, exposing the two clastic dikes. BPF 3 detected pressure changes perpendicular to the entry and showed a total increase of approximately 35 psig in the first day, while BPF 4 bled off (fig. 17). Some natural bleedoff is expected as the hole deforms if there is no movement in the roof to apply pressure to the BPF or if extension occurs in the beam of the roof. By the second day, U-cell 1 (closest to the inby rib) showed an increase in load of nearly 290 psig as a cutter began to develop along the inby rib between the clastic dikes intersecting the rib (fig. 18). From past experience with cutters developing this quickly, it was suggested that supplemental support be installed immediately. Trusses were installed between the rows of bolts (day 3), resulting in an immediate decrease in the rate of loading (fig. 19). The addition of trusses effectively reunited the natural beam of the roof and prevented the roof from deteriorating further. Finally, loading leveled off and the cutter did not become any more severe. Figure 20 summarizes the maximum load seen by each U-cell in the crosscut. Once again, the loading roughly paralleled that which would occur from a cantilever beam.

In the next area (fig. 15*C*) trusses were being used on a regular basis and had been successful in deterring the formation of cutters. Shortly after this cut was mined, some rock did fall from the clastic dike in the roof, but this activity ceased once trusses were installed. Figure 21 shows the total loading seen by each U-cell across the entry.

FIGURE 19.—Example of roof trusses supporting cutter roof.

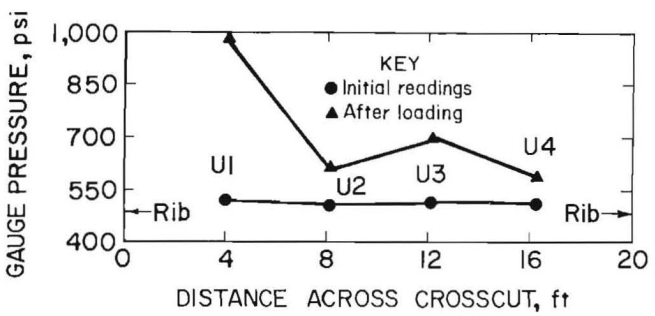

FIGURE 20.—Initial and maximum loads for U-cells 1-4 across the crosscut shown in figure 15*B* (*8*).

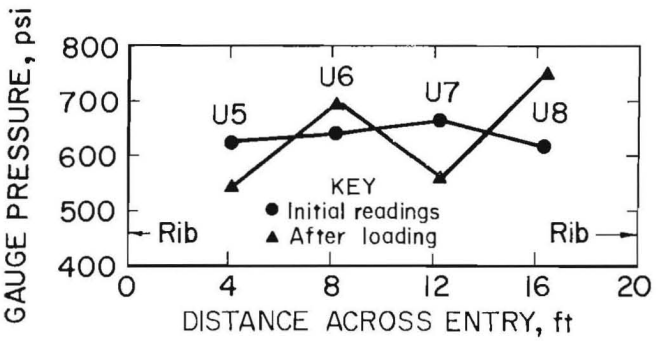

FIGURE 21.—Initial and maximum load changes for U-cells 5-8 across the entry shown in figure 15*C* (*8*).

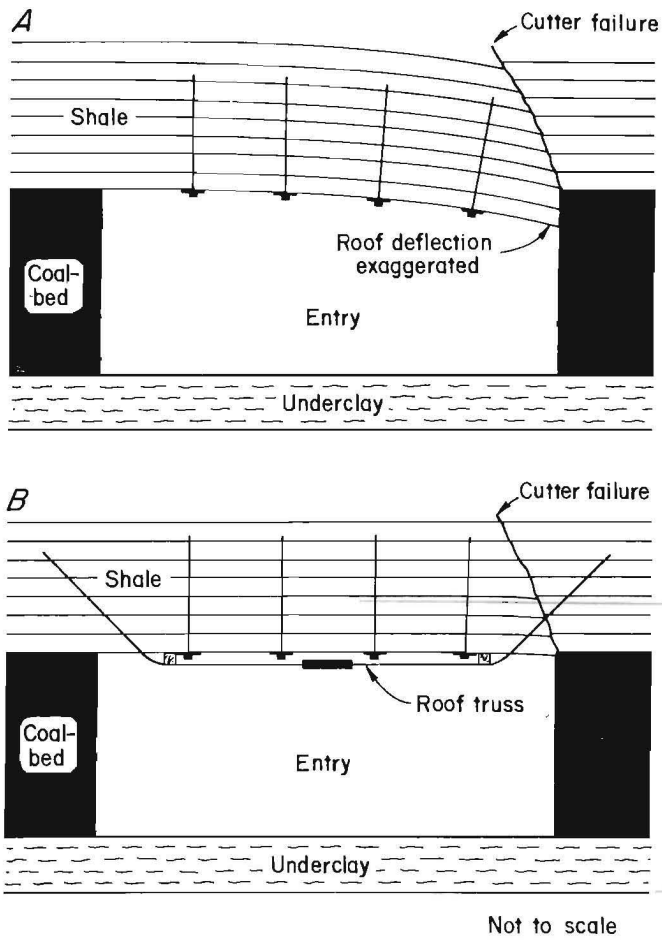

FIGURE 22.—Schematic of roof movement (cantilever beam) before and after installation of roof trusses.

Very little loading occurred on U-cells 6 and 8, while U-cells 5 and 7 actually bled off. Bleedoff of loading on bolts is natural if there is no new inducement of load (17). Figure 22 depicts what is suspected to be happening prior to and after roof truss installation. Just after mining and exposure of a clastic dike, the roof begins to sag, loose roof rock falls, and cutter failure initiates (fig. 22*A*). After the trusses are installed, the clastic dike, cutter, and roof fractures are partially closed by the upward thrust and compressive forces transmitted to the strata by the trusses (18) (fig. 22*B*). Further roof movement and cutter formation are deterred by the introduction of shear strength across the plane of fracture, as witnessed by the absence of additional bolt loading.

Steel-fiber-reinforced concrete cribs were monitored using flat hydraulic cells as shown in figure 23. Figure 24 shows the crib loading detected by two flat cells for approximately 3 months. Flat cell 2 was installed on a crib that eventually was overridden by a cutter. The large increase in load it measured resulted from the cantilever beam effect (roof deflection) as the cutter developed.

IN SITU STRESS MEASUREMENTS

The final task of the Main A investigation was the measurement of the in situ horizontal stress in the mine roof. These measurements were needed to determine if high horizontal roof stresses were contributing to cutter formation. The Council for Scientific and Industrial Research Strain Gauge Strain Cell (Doorstopper) system was used to measure the stresses.[3] The Doorstopper consists of a strain gauge rosette (four strain gauges at -45°, 0°, +45°, and +90°) molded into a rubber casting which fills a plastic shell. The stress in the rock is measured using an overcoring stress-relieving technique; subsequently, the stress at the end of a flattened borehole is related to the stresses in the surrounding rock (19).

[3]Reference to specific products does not imply endorsement by the Bureau of Mines.

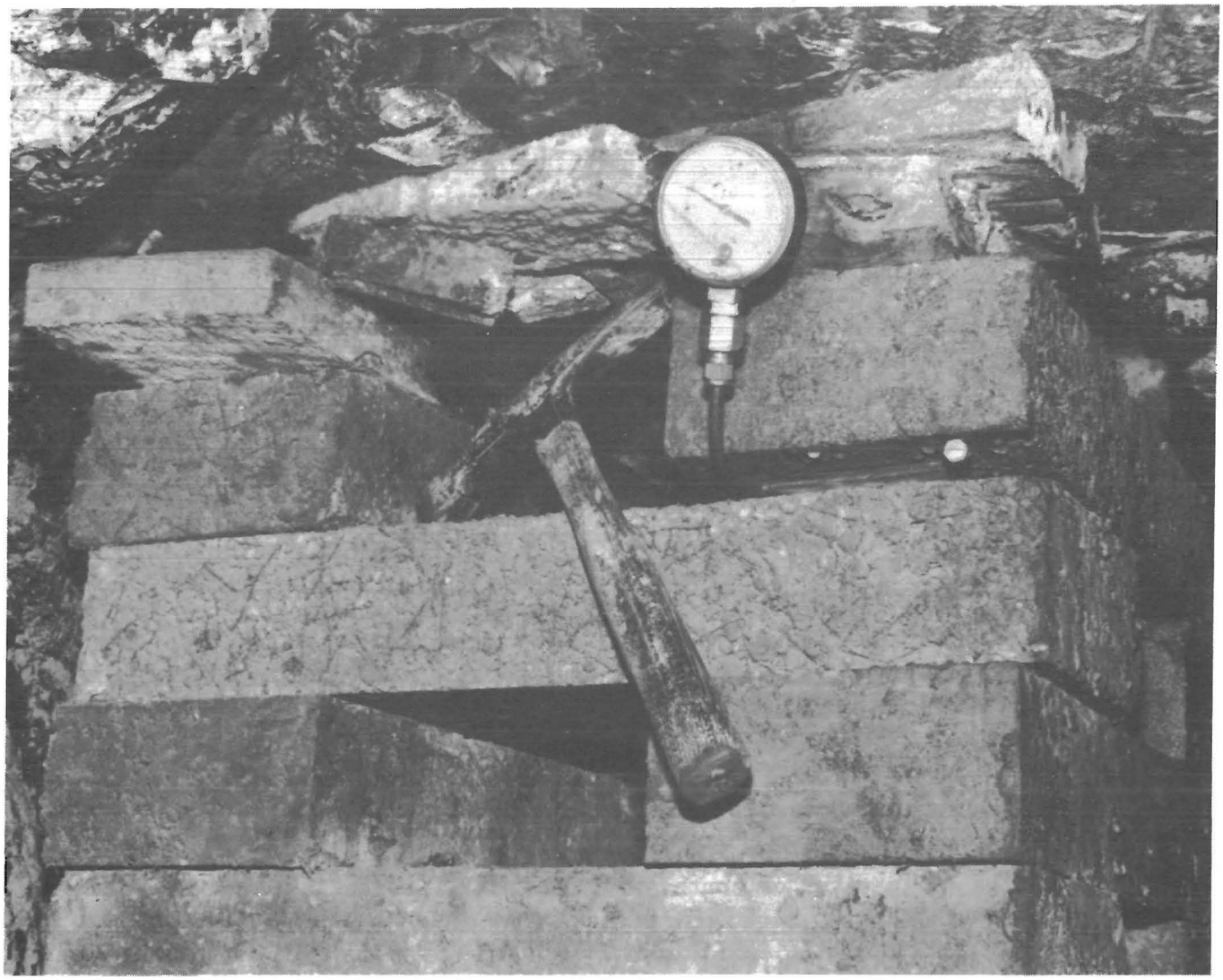

FIGURE 23.—Flat hydraulic cell monitoring loading on a steel-fiber-reinforced concrete crib.

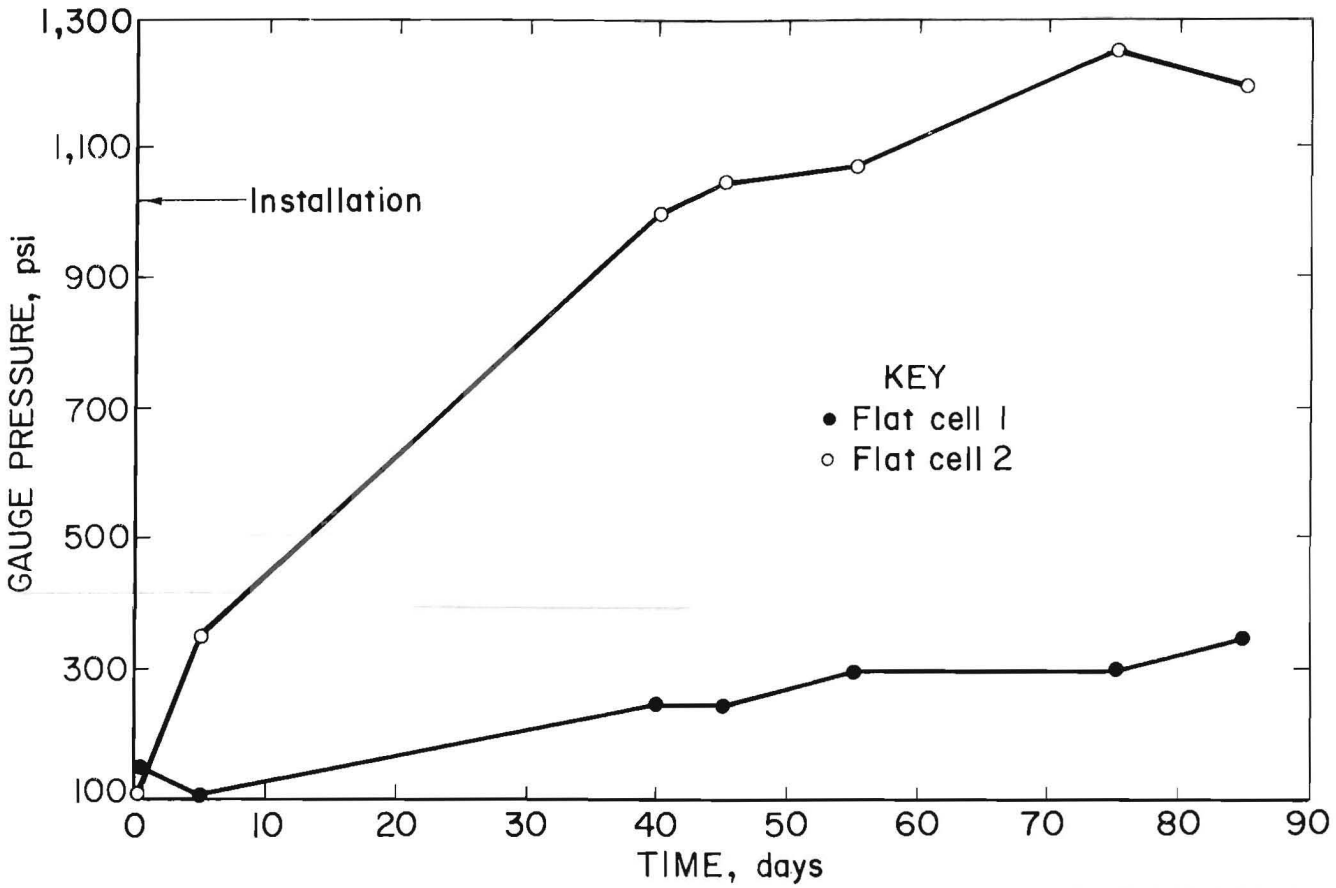

FIGURE 24.—Crib load monitoring behavior of flat cells 1 and 2.

TABLE 3. - Results of in situ horizontal roof stress measurements

Cell	Height above coal, ft	Max compressive stress, psi[1]	Orientation[1]
1.....	16.75	620	N 69° W
2.....	18.67	509	N 79° W
3.....	20.58	305	N 76° W
4.....	21.33	497	N 36° W

[1]Calculated using a tangent Young's modulus of 2.01×10^6 and a tangent Poisson's ratio of 0.33.

The site, adjacent to corehole 2, was selected because of its proximity to the mine areas experiencing the most cutter failure (fig. 6). Four complete measurements were made at depths from 16.75 to 21.33 ft into the mine roof. The results are summarized in table 3 and figure 25.

In general, the measured stresses appear insufficient to initiate cutter failure on their own. They have, however, influenced the angle of fracture propagation into the roof. The ratio of horizontal stress to vertical stress will dictate the inclination of the plane of

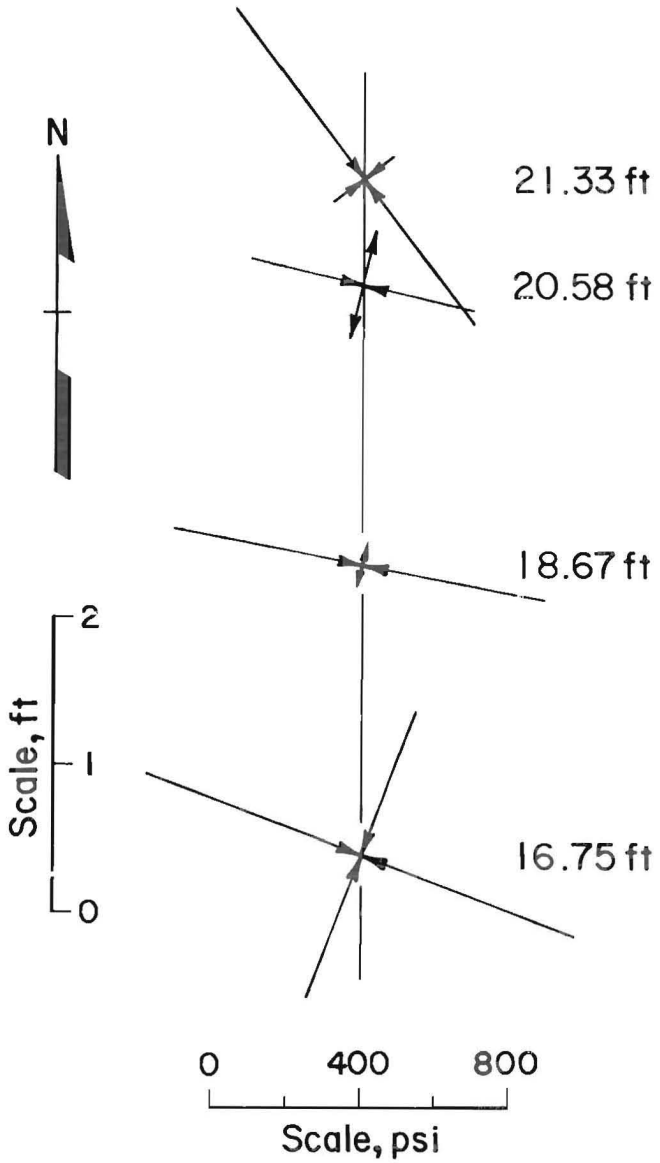

FIGURE 25.—Vector plot in situ horizontal roof stress measurements. Feet is depth into the mine roof. North arrow for reference to orientation of stress measurements.

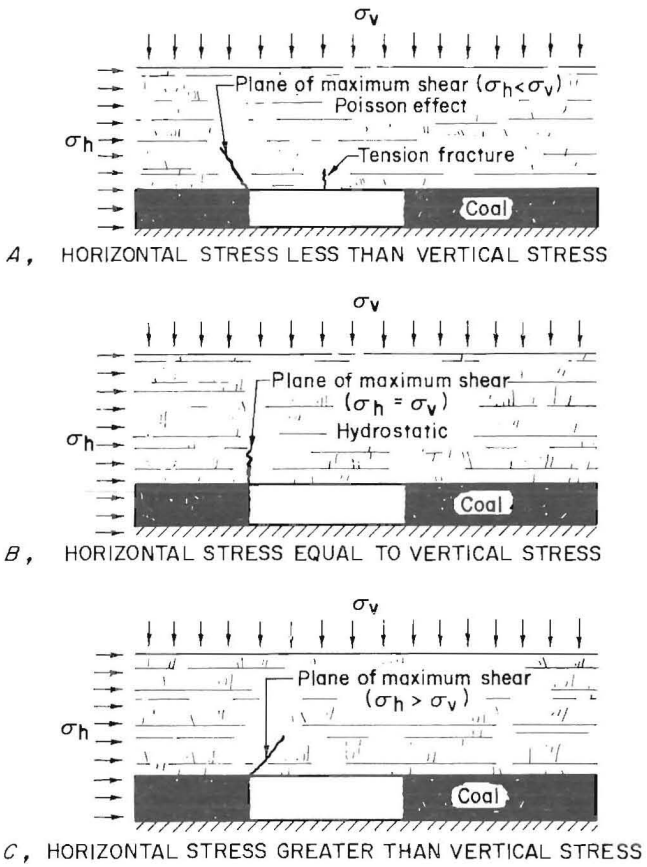

FIGURE 26.—Qualitative example of the influence of the horizontal stress to vertical stress on the angle of failure propagation (7).

failure (fig. 26). At the test site the estimated vertical stress, based on overburden load only, is approximately 450 psi. The measured horizontal stress ranged from 305 to 620 psi, indicating the failure angle should be nearly vertical or slightly inclined out over the entries. Underground observations of cutter failure and roof falls have shown this to be the case. At some time in the past the horizontal stress may have been greater than what was measured and would have had a significant impact on cutter failure, but it is likely that some stress relieving has occurred during entry development. The most logical reason for the stress relief is that the numerous fractures and roof falls near the test site have provided avenues for the strata to move and release the in situ stresses.

ROOF FAILURE ANALYSIS

Observations made during mapping revealed that cutters mainly formed adjacent to clastic dikes shortly after mining. This suggested that the disruption of roof integrity, due to the presence of clastic dikes, contributed to the propagation of cutters. The natural beam of the roof rock, spanning from pillar to pillar, is severed when a clastic dike is present, causing the roof to behave as a cantilever beam (fig. 27). In most cases, the cutters formed at the obtuse angle of the clastic dike-rib intersection, propagating inby or outby depending on the situation. They initiate at this location because it is where the maximum load on the beam occurs and thus is the most susceptible failure point.

Simply stated a cantilever beam has one end free while the other is fixed, with maximum deflection occurring at the free end and maximum vertical shear forces at the hinged end (fig. 28) (20). Applying this principle to cutter roof failure, as a cutter forms at one roof-rib intersection (clastic dike-rib intersection), the free end of the beam is created. The fixed end is found at the other roof-rib intersection. As the free end of the roof beam deflects downward, internal stresses develop. When the roof is considered to be a series of thin plates, with only friction between the layers to resist movement, shear slip will develop along fractures and bedding planes, parallel to the beam, with the maximum

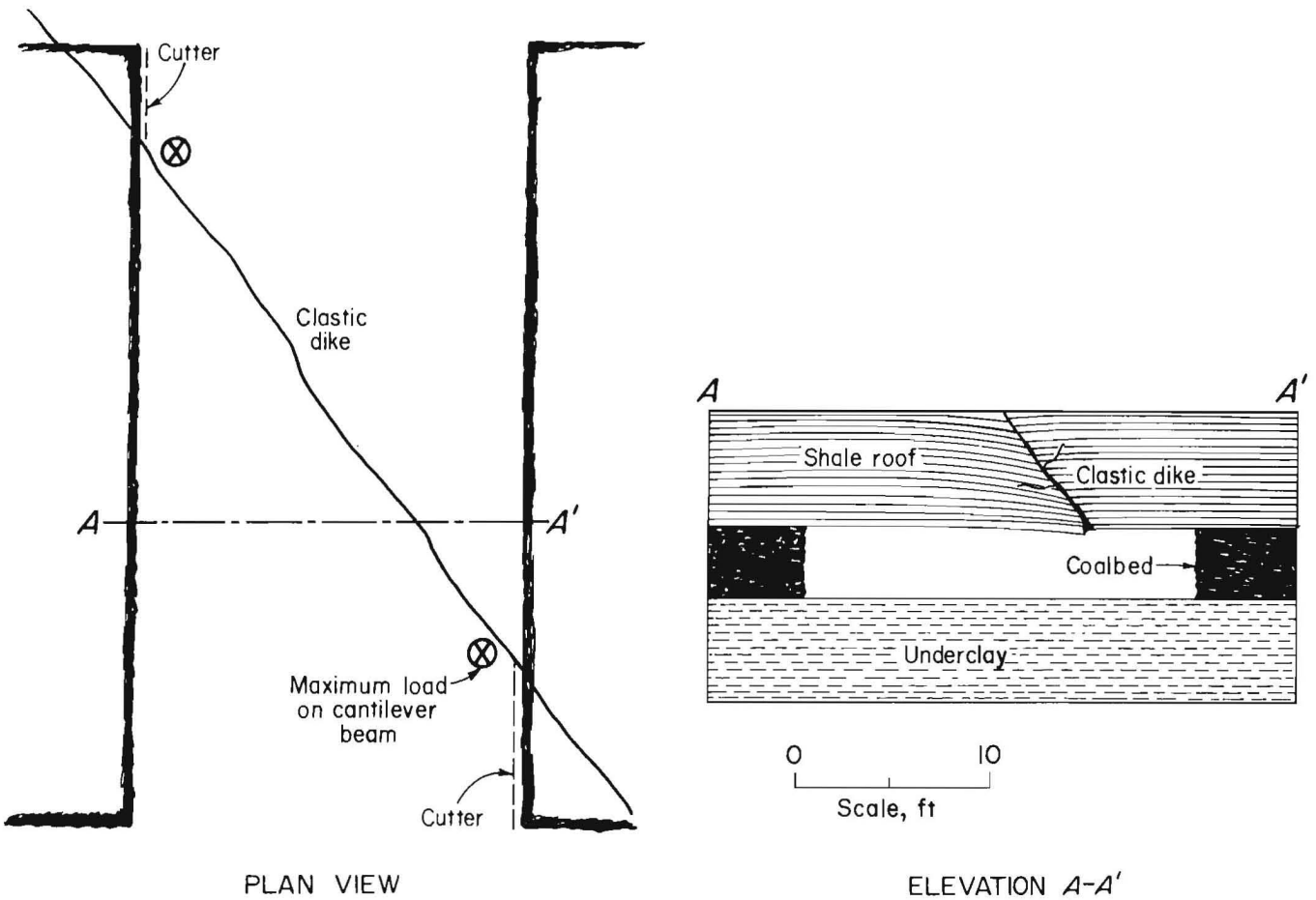

FIGURE 27.—Schematic of cantilever beam effect that occurs during cutter roof failure (8).

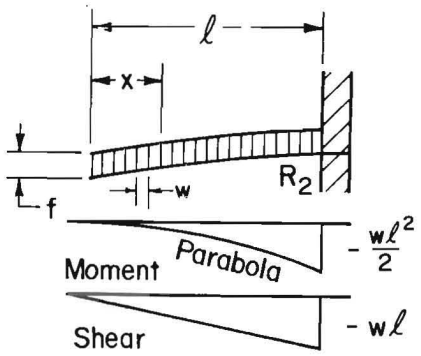

Reaction $(R_2) = W = w\ell$

Bending moment $(M_x) = -\frac{wx^2}{2}$

Maximum bending moment $(M_{max}) = -\frac{w\ell^2}{2}, (x = \ell)$

Total vertical shear $(Q_x) = -wx$

Maximum vertical shear $(Q_{max}) = -w\ell, (x = \ell)$

Deflection $(f) = \frac{W}{EI}\frac{\ell^3}{8}$ (max)

Weight of individual beam cross section = w

Total weight of beam = W

FIGURE 28.—Beam deflection diagram for a cantilever beam subjected to a uniformly distributed load (19).

horizontal shear slip at the free end of the beam (fig. 29) (21-22). An increase in bolt loading (tension) will be induced by the shear slip only, because the bolts do not extend through the beam and into the solid roof above.

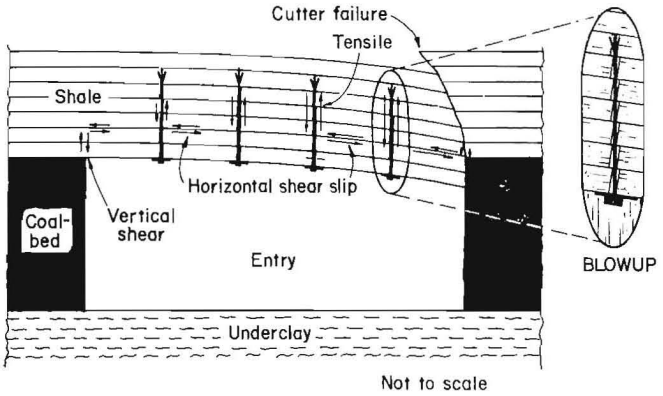

FIGURE 29.—Schematic of forces in roof strata subject to cantilever beam failure.

This cantilever beam scenario was evident in the results of the rock pressure monitoring. Increased bolt loading was measured as cutter failure progressed, with the maximum increase found next to the cutter (the free end of the beam where the shear slip was greatest). Decreased loading was detected after trusses were installed, a result of reducing the shear slip by eliminating some of the downward deflection of the cantilever beam. Additionally, the pressure increases in the roof strata measured by BPF's were indicative of a cantilever beam. The BPF's were detecting the shear slip along the bedding planes parallel to the beam. Thus all measurements and observations support the contention that the roof is failing as a cantilever beam.

DETAILED GEOLOGIC MAPPING OF NORTH AND SOUTH MINES

Prior to, during, and after the Main A investigation, company personnel and a private consultant conducted detailed geologic mapping of the North and South Mines. The features recorded included clastic dikes, cutters, roof falls, slips, faults, kettlebottoms, joints, floor heave, coal cleat, and roof rock lithology. A few of the significant results from the mapping of the North and South Mines follow:

1. The characteristics of the clastic dikes were similar to those found earlier during the Main A investigation; see "Assessment of Ground Conditions" section for a detailed description of clastic dike characteristics.

2. In areas overlain by channel and splay sandstones, the dikes were filled with a number of sediments in addition to claystone and coal, including fine sand and silt.

3. Cutters developed where no dikes were present, and there were areas where numerous dikes were present with no cutter development.

4. The clastic dikes mapped throughout the remainder of the North and South Mines appear to be somewhat more random in orientation than was found during the mapping of the much smaller Main A area.

CONCLUSIONS

The increased occurrence of cutter roof failure in the Main A headings was attributed to the high frequency of clastic dikes. Clastic-dike-disturbed roof had a higher fracture frequency (lower RQD value) and thus was more prone to failure. Rock and support pressure monitoring near clastic dikes revealed that the roof strata were behaving as a cantilever beam because the dikes were "severing the roof beam." This cantilever action initiated cutter failure, which developed along entries or crosscuts, often extending across several breaks. Locations where two or more clastic dikes intersect proved to be the areas most susceptible to cutter roof failure. Horizontal roof stresses were shown to be insufficient to initiate cutter failure, but in combination with the clastic dikes, have promoted cutter failure and dictated the angle of fracture propagation into the roof.

Finally, the correlation between clastic dikes and cutter roof failure was distinctive to the face area of Main A only. The interactions of clastic dikes and cutter failure in the remaining mine areas were not, in all cases, similar to those observed in the Main A headings.

REFERENCES

1. Aggson, J. R. Stress-Induced Failures in Mine Roof. BuMines RI 8338, 1979, 16 pp.

2. Kripakov, N. P. Alternatives for Controlling Cutter Roof in Coal Mines. Paper in Proceedings of the Second Conference on Ground Control in Mining. WV Univ., Morgantown, WV, 1982, pp. 142-151.

3. Thomas, E. Conventional Timbering Versus Suspension Supports. Paper in Proceedings: Fifth International Conference of Directors of Mine Safety Research, comp. by H. P. Greenwald. BuMines B 489, 1950, pp. 175-183.

4. Moebs, N. N., and J. L. Ellenberger. Geologic Structures in Coal Mine Roof. BuMines RI 8620, 1982, 16 pp.

5. Iannacchione, A. T., J. T. Popp, and J. A. Rulli. The Occurrence and Characterization of Geologic Anomalies and Cutter Roof Failure: Their Affect on Gateroad Stability. Paper in Stability in Underground Mining (Proc. 2d Int. Conf., Lexington, KY, Aug. 6-8, 1984). Soc. Min. Eng. AIME, 1984, pp. 428-445.

6. Chase, F. E. Clay Veins: Their Physical Characteristics, Prediction, and Support. Paper in Proceedings of the Fourth Conference on Ground Control in Mining. WV Univ., Morgantown, WV, 1985, pp. 212-219.

7. Hill, J. L., III. Cutter Roof Failure: An Overview of the Causes and Methods for Control. BuMines IC 9094, 1986, 27 pp.

8. Hill, J. L. III, and E. R. Bauer. An Investigation of the Causes of Cutter Roof Failure in a Central Pennsylvania Coal Mine: A Case Study. Paper in Rock Mechanics in Productivity and Protection, Twenty-Fifth Symposium on Rock Mechanics (Northwestern Univ., Evanston, IL, June 25-27, 1984). Soc. Min. Eng. AIME, 1984, pp. 603-614.

9. _____. Computer Application to Roof Rock Quality Analysis. Paper in Proceedings of the Second Conference on the Use of Computers in the Coal Industry. Univ. AL, Tuscaloosa, AL, 1985, pp. 311-316.

10. Deere, D. U. Technical Description of Rock Cores for Engineering Purposes. Roch Mech. and Eng. Geol., v. 1, No. 1, 1964, pp. 17-22.

11. Kalia, H. N. Improving the Design of Coal Mines by Borehole Logging, Rock Mechanics, and Related Data. Soc. Min. Eng. AIME preprint 73F72, 1973, 5 pp.

12. Broch, E., and J. A. Franklin. The Point Load Strength Test. Int. J. Rock Mech. and Min. Sci., v. 8, No. 9, 1972, pp. 669-697.

13. Bauer, R. A. The Relationship of Uniaxial Compressive Strength to Point-Load and Moisture Content Indices of Highly Anisotropic Sediments of the Illinois Basin. Paper in Rock Mechanics in Productivity and Protection, Twenty-Fifth Symposium on Rock Mechanics (Northwestern Univ., Evanston, IL, June 25-27, 1984). Soc. Min. Eng. AIME, 1984, pp. 398-405.

14. Fitzhardinge, C. F. R. Note on the Point-Load Strength Index Test. Aust. Geomech. J., v. 68, No. 6, 1978, 53 pp.

15. Wang, F. D., D. M. Ropchan, and M. C. Sun. Proposed Technique for Improving Coal-Mine Roof Stability by Pillar Softening. Trans. Soc. Min. Eng. AIME, v. 255, 1974, pp. 59-63.

16. Bauer, E. R., G. J. Chekan, and J. L. Hill III. A Borehole Instrument for Measuring Mining-Induced Pressure Changes in Underground Coal Mines. Paper in Research and Engineering Applications in Rock Mechanics, Twenty-Sixth Symposium on Rock Mechanics (SD Sch. Mines and Technol., Rapid City, SD, June 26-28, 1985). A. A. Balkema, Accord, MA, 1985, pp. 1,075-1,084.

17. Roberts, M. New Roof Bolt Passes U.S. Tests. Coal Age, v. 85, No. 7, 1980, pp. 122-127.

18. Peng, S. S. Coal Mine Ground Control. Wiley, 1978, pp. 420-422.

19. Roctest, Inc. (Plattsburgh, NY). CSIR Strain Gauge Strain Cell ("Doorstopper") Instruction Manual. 1985, 17 pp.

20. Timoshenko, S. P., and J. M. Gere. Mechanics of Materials. Van Nostrand, 1972, p. 95.

21. Jeffrey, R. G., and J. J. K. Daemen. Analysis of Rockbolt Reinforcement of Layered Rock Using Beam Equations. Paper in Proceedings of the International Symposium on Rock Bolting. A. A. Balkema, 1983, pp. 173-185.

22. Hanna, K., D. Conover, K. Haramy, and R. Kneisley. Structural Stability of Coal Mine Entry Intersections - Case Studies. Paper in Rock Mechanics : Key to Energy Production, Twenty-Seventh Symposium on Rock Mechanics (Univ. AL, Tuscaloosa, AL, June 23-25, 1986). Soc. Min. Eng. AIME, 1986, pp. 512-519.

U.S. GOVERNMENT PRINTING OFFICE: 1987 - 605-017/60085

INT.-BU.OF MINES,PGH.,PA. 28550